Experimental Mechanics (2018) 58:487–497
https://doi.org/10.1007/s11340-017-0366-z

Strain-Rate-Dependent Yield Criteria for Progressive Failure Analysis of Composite Laminates Based on the Northwestern Failure Theory

J.D. Schaefer[1] · I.M. Daniel[2]

Received: 9 July 2016 / Accepted: 7 December 2017 / Published online: 10 January 2018

Abstract
The strain-rate-dependent failure of a fiber-reinforced toughened-matrix composite (IM7/8552) was experimentally characterized over the range of quasi-static (10^{-4} s^{-1}) to dynamic (10^{3} s^{-1}) strain rates by testing off-axis lamina and angle-ply laminate specimens. A progressive failure framework was proposed to describe the matrix-dominated transition from linear elastic to non-linear material behavior as determined from the experimentally measured stress-strain material response, and the Northwestern Failure Theory was adapted to provide a set of apparent yield criteria for predicting the matrix-dominated yielding of composites using the lamina-based transverse tension (F_{2t}^{y}), transverse compression (F_{2c}^{y}), and in-plane shear (F_{6}^{y}) yield strengths. The underlying theory was validated by determining the applicability of the new damage-mode-based yield criteria. Starting with the lamina, the proposed criteria accurately predicted the matrix-dominated yielding. Angle-ply laminates were then investigated to isolate the matrix-dominated laminate behavior based on fiber orientation, and the predictions were found to be in superior agreement with the experimental results compared to the classical failure theories. The results indicate the potential of using the Northwestern Yield and Failure Criteria to provide the predictive baseline for damage propagation from yield to ultimate lamina failure in composite laminates.

Keywords Damage mechanics · Lamination theory · Polymer-matrix composites · Non-linear behavior · Progressive damage analysis

Introduction

Composite failure at the structural scale is designed to be a controlled process comprised of scale-relevant phenomena. Proper implementation of computational models for predicting damage initiation and propagation to ultimate failure for the various (and interacting) matrix and fiber-dominated mechanisms must be completed with an understanding of the direct model outputs to be correlated with experiments. Furthermore, effective model validation is only achieved when the approach is demonstrated to accurately predict the damage phenomena at multiple levels of the component hierarchy [1].

While numerous capabilities exist for modeling fiber-dominated material behavior, it is increasingly clear that the application of classical approaches for predicting matrix damage in composite laminates remains a challenge [2]. The inability of classical theories to accurately predict ultimate lamina failure (two-piece) is a critical concern for numerical analysis which requires a fundamental criteria for predicting embedded ply failure in complex composite laminates (i.e. progressive failure). It is proposed that any investigation of progressive ply failure in composite laminates first accurately predict in-situ layer failure initiation so that the damage propagation models may be effectively implemented.

In light of this 'progressive damage and failure' framework, it is critical to determine not only when a lamina or laminate fails, but when it *begins* to fail (e.g. when first damage occurs). In the current work, matrix yielding is defined as the initiation of the failure process in composite laminates as experimentally measured from the characterized stress-strain curves for off-axis lamina and angle-ply laminate specimens. Macroscopically, the yield point is the point at which the

✉ J.D. Schaefer
joseph.d.schaefer@boeing.com

I.M. Daniel
imdaniel@northwestern.edu

[1] The Boeing Company, 6300 James S McDonnell Blvd, Berkeley, MO 63134, USA

[2] Northwestern University, 2137 Tech Drive, Evanston, IL 60208-3020, USA

stress-strain behavior breaks linearity, which is typically measured experimentally as the transition from linear to non-linear response (ASTM D695, Section 3.2.7/11.4). In structural design, the yield point is typically identified by a prescribed offset value. In the current work, the yield point is identified as the first measured change in material response from the stress-strain curve as defined in ASTM D695 practically encapsulate damage mechanisms below the scale of direct measurement at the lamina length scale (e.g. micro-cracks, plasticity, etc.) which is generally modeled using continuum mechanic approaches. The yield point for an off-axis 75° lamina specimen tested in compression is shown in Fig. 2. The yield point represents the point at which stress and strain may be accurately determined utilizing a linear elastic analysis to predict failure for non-linear materials. Beyond the yield point, the stress predicted by linear elastic failure models no longer correlates with the actual material strain. Importantly, this discrepancy may lead to a significant and propagating error when such approaches are used to model the progressive failure of composite laminates; thus, evaluation and quantification of model uncertainty becomes ambiguous. For composite laminates, the need exists to define the point at which composite damage is initiated, how this damage progresses towards isolated ply failure, and how the multiple ply failures propagate to cause ultimate catastrophic laminate failure on a length scale relevant basis. It is necessary to have criteria by which damage is predicted to initiate prior to ultimate lamina failure in order for potential matrix non-linearity to be effectively modeled and validated. A framework based on linear elastic response, yielding, pre-peak nonlinearity, failure criteria, and post-peak response has recently been developed by Razi and Schaefer for practical validation of analysis formulation at the level of the representative unit cell (e.g. finite element) for structural analysis [3].

Table 1 Lamina compressive axial yield stresses at quasi-static, intermediate, and dynamic strain rates

$[\theta]_{54}$	10^{-4} s^{-1} (MPa) [Std. Dev]	1 s^{-1} (MPa) [Std. Dev]	300–1000 s^{-1} (MPa) [Std. Dev]
90	105 [5]	146 [5]	175 [2]
75	100 [3]	144 [8]	168 [8]
60	100 [5]	137 [5]	170 [3]
45	96 [5]	135 [8]	170 [3]
30	116 [14]	154 [4]	178 [14]
15	170 [9]	224 [5]	246 [20]

The Northwestern Yield Criteria are introduced as the theoretical basis for predicting matrix-dominated yield behavior in composites. Sub-component validation is addressed through investigation of the matrix-dominated failure modes in composite lamina. The investigation then extends to the component case of angle-ply laminates wherein thermally-induced residual stresses are present. The Northwestern Yield Criteria are presented as strain-rate-dependent criteria for determining the yielding of composite laminates, both lamina and angle-ply, over applicable ranges of loading rate. This work serves to provide an accurate representation of the elastic behavior of matrix-dominated layups to potentially enhance the analysis implementation of computational solid mechanics approaches. Such criteria may be used within the formulation for finite elements to (via a UMAT/VUMAT/UEL) to signal the start of stiffness degradation prior to element failure [3].

Lamina Failure

The Hexcel IM7/8552 material system was selected for this work. IM7/8552 is a popular research medium for aerospace

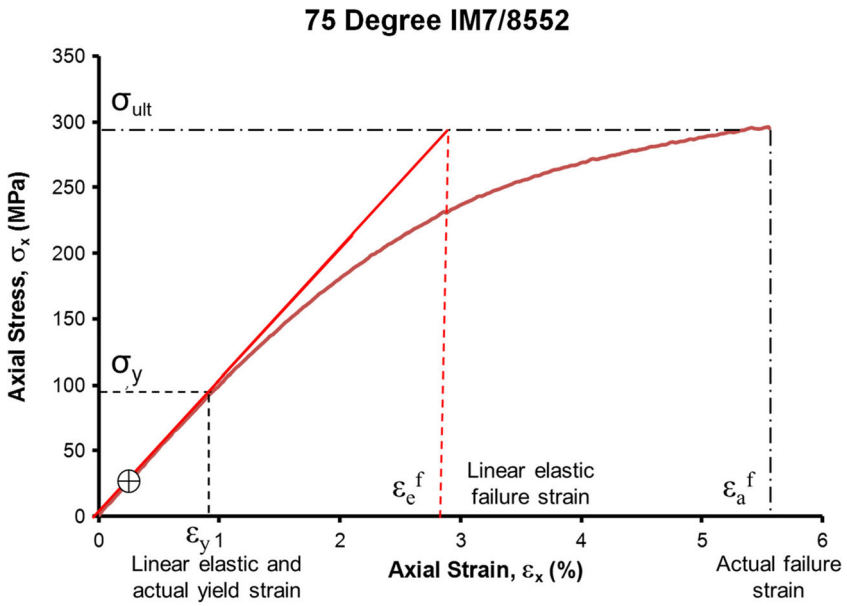

Fig. 1 Stress-strain curve of a 75 deg. off-axis lamina under compression illustrating lamina yielding and ultimate failure; moduli measured between 2000 μstrain and yield point

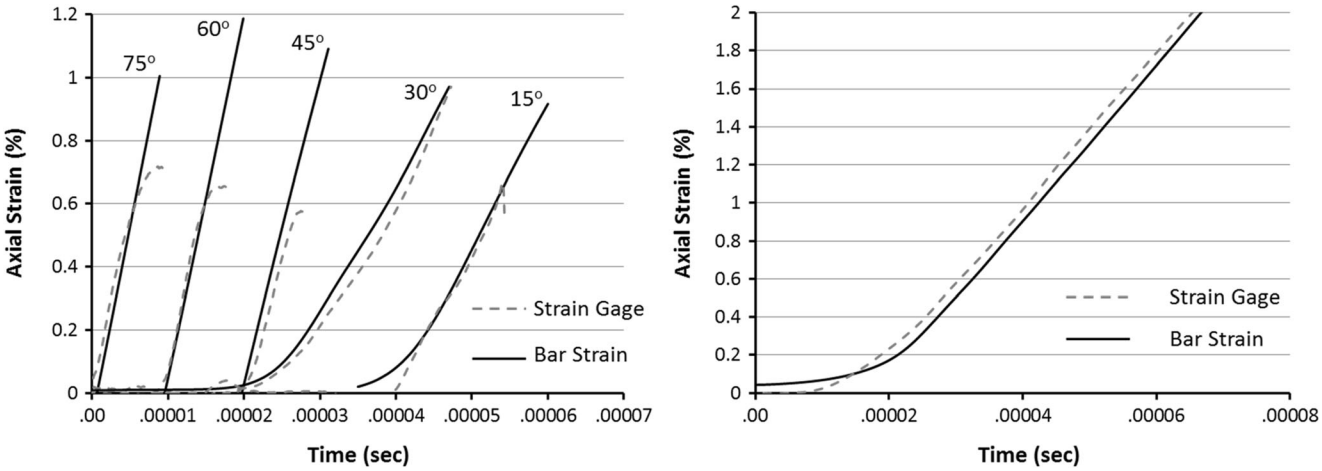

Fig. 2 Bar calculated and strain gage initial strain-time histories for off-axis lamina (left) and ±45° angle-ply (right)

applications [4–11] and has been qualified and characterized by NCAMP [12]. Hexply® 8552 prepreg is an amine cured, toughened resin system and was provided as a 48 in. wide roll with the fibers aligned along the rolling direction. The epoxy resin was toughened with a thermoplastic polymer that provides the material with increased damage resistance and increased strain to failure; thus, considerable non-linear response under loading is present for certain ply layups.

Developed by Daniel et al. [13], the Northwestern University (NU) Theory is a failure mode based failure theory derived from the matrix behavior at the micro-scale of composites yet expressed in terms of macroscopic material properties. As noted by the authors, the NU criteria are suitable for interfiber and interlaminar failure under transverse normal, and parallel to the fibers shear loading on the 1–2 or 1–3 planes. The criteria are especially applicable to highly anisotropic composites with failure occurring due to a low interaction of modes. It was previously found that the NU Theory performs quite well at predicting the ultimate matrix-dominant failure of both unidirectional and fabric composites [13–17].

Northwestern Yield Criteria

The Northwestern Failure Theory (NU Theory) for Composites was recast as a set of yield criteria based on transverse tensile, transverse compression, in-plane shear yield, transverse modulus, and in-plane shear modulus (F_{2t}^{y}, F_{2c}^{y}, F_{6}^{y}, E_2, and G_{12}). The underlying NU Theory formulation remains the same [13]; however, the noted yield properties were substituted for the previously used ultimate lamina failure values:

$$\left(\frac{\sigma_2^*}{F_{2c}^y}\right)^2+\left(\frac{E_2}{G_{12}}\right)^2\left(\frac{\tau_6^*}{F_{2c}^y}\right)^2=1 \quad \text{Compression Dominated Yield}$$

$$\left(\frac{\tau_6^*}{F_6^y}\right)^2+2\left(\frac{G_{12}}{E_2}\right)\left(\frac{\sigma_2^*}{F_6^y}\right)=1 \quad \text{Shear Dominated Yield}$$

$$\left(\frac{\sigma_2^*}{F_{2t}^y}\right)+\frac{1}{4}\left(\frac{E_2}{G_{12}}\right)^2\left(\frac{\tau_6^*}{F_{2t}^y}\right)^2=1 \quad \text{Tension Dominated Yield}$$

where σ_2^* and τ_6^* are a function of strain rate.

In terms of progressive failure, the NU Yield Criteria (NU Yield) essentially provide the basis for predicting when damage occurs according to a specific underlying matrix dominated mode; thus, the NU Yield Criteria are treated as a set of 'damage' criteria.

Table 2 Strain-rate-dependence of NU Criteria lamina properties

Property	10^{-4} s^{-1}	1 s^{-1}	300–1000 s^{-1}
Transverse Modulus, E_2 (GPa)	9	10.6	11.2
Shear Modulus, G_{12} (GPa)	5.6	6.2	6.8
Transverse Tensile Yield, F_{2t}^{y} (MPa)	41 [2]	51 [3]	(66)
Transverse Compressive Yield, F_{2c}^{y} (MPa)	105 [5]	146 [5]	175 [2]
Shear Strength, F_{6}^{y} (MPa)	39 [3]	50 [3]	(61)

Strain-Rate-Dependent Lamina Yielding

Further complicating the analysis of composite materials is the tendency for the matrix-dominated properties to be influenced by strain rate [14]. Due to their brittle nature and propensity for defect-driven length-dependent failure, it is assumed that carbon fibers exhibit insignificant strain rate sensitivity. Werner et al. [16] recently performed extensive characterization of matrix constituent property dependence on strain rate and developed constitutive relations of the material under biaxial states of stress. The influence of strain rate on composite materials has become a considerably active area of investigation [15, 17–21].

In the current work, the experimental lamina data was previously obtained by Schaefer et al. [17]. From this work, the yield points for off-axis lamina specimens ($\theta = 15 - 90^o$) tested in uniaxial compression were determined as shown in Fig. 1 for each tested strain rate. The

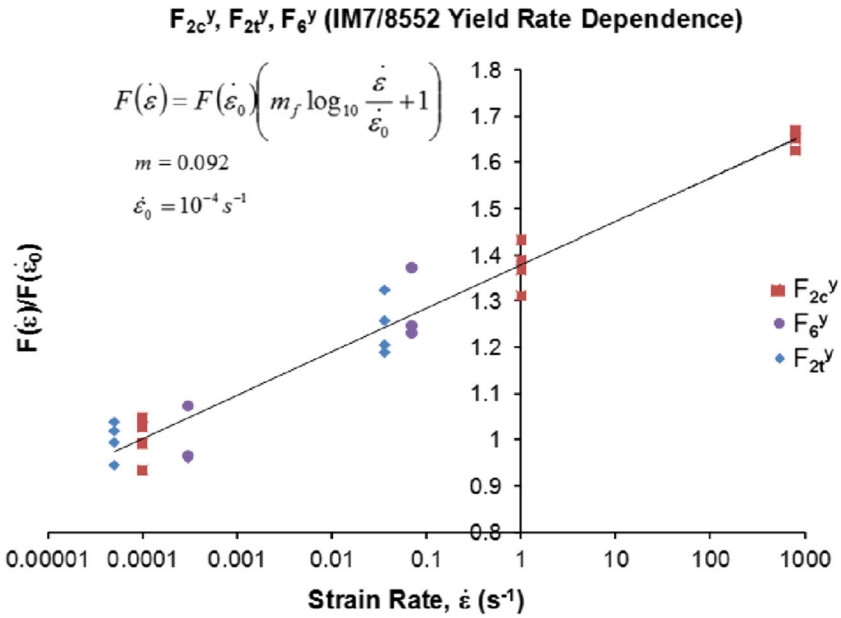

Fig. 3 Strain-rate-dependence of yield properties (F_{2c}^{y}, F_{2t}^{y}, and F_6^{y})

moduli were determined by the chord modulus technique between 2000 μstrain and the noted yield point for each test (noted in Fig. 1). The off-axis fiber orientation to the loading direction induces a state of biaxial compressive and in-plane shear stress in the specimen. The average values are provided in Table 1. Previously, Werner et al. [16, 22], and Schaefer et al. [23] investigated dynamic strain rate bar characteristics based on impedance, drive pressure, and bar diameter to minimize required ring-up time. For the off-axis and angle-ply specimens tested in the current work, the ring-up time was estimated to be less than 5% of the total test duration. Axial strain gages were affixed to the specimen surface to measure the strain-time response during the initial portion of the dynamic loading event during split Hopkinson bar testing. Shown in Fig. 2, the initial strain-time histories for the bar-calculated and strain gage strains are observed to correlate well.

The five average lamina properties used in the NU Yield Criteria (F_{2t}^{y}, F_{2c}^{y}, F_6^{y}, E_2, and G_{12}) are shown in Table 2 for each tested strain rate.

In the table, the properties are shown to increase with increasing strain rate. As previously presented [17], the values for shear strength and transverse tension at the dynamic strain rate were obtained by extrapolation of the data trend, which was established by plotting the individual test values for F_{2c}^{y}, F_{2t}^{y}, and F_6^{y} against the logarithm of strain rate (Fig. 3). While

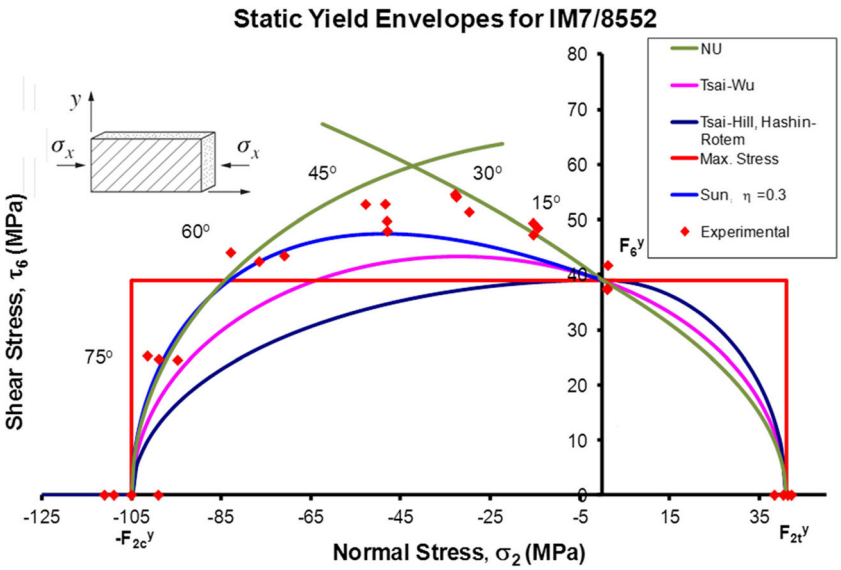

Fig. 4 Comparison of static yield envelopes for IM7/8552

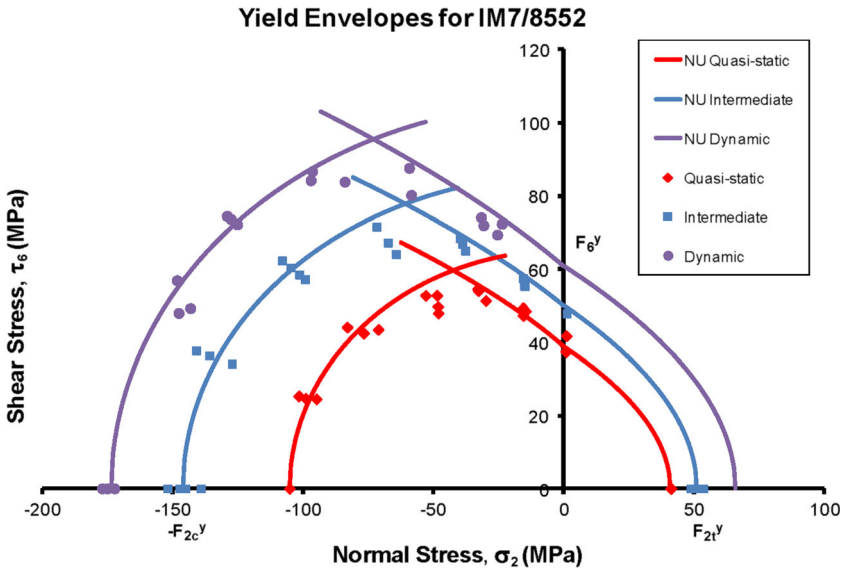

Fig. 5 NU Yield envelopes for quasi-static, intermediate, and dynamic strain rates

not a measured value, the proposed estimate values provide the opportunity for further validation testing.

The data was fitted with a relationship linear in the log of strain rate:

$$F^y(\dot{\varepsilon}) = F^y(\dot{\varepsilon_o})\left[m\log_{10}\left(\frac{\dot{\varepsilon}}{\dot{\varepsilon_0}}\right)+1\right] \quad (1)$$

where F^y is the yield stress ($F_{2c}^{\ y}$, $F_{2t}^{\ y}$, $F_6^{\ y}$), m is 0.092, and $\dot{\varepsilon_o}$ is reference strain rate of 10^{-4} s^{-1}.

The yield property strain rate dependence represented by the slope $m = 0.092$ was found to be higher than that for the unidirectional lamina ultimate failure ($m = 0.055$) [17]. In terms of material properties, the matrix yield strength is considerably lower than that of the brittle fibers; thus, the yield strength strain-rate-dependence for the unidirectional off-axis lamina is expected to coincide with that of the matrix for matrix-dominated layups. From equation (1), the stresses were normalized by the corresponding values at the reference strain rate, $\dot{\varepsilon_o}$, according to the relation:

$$f^y(\dot{\varepsilon}) = \left[m\log_{10}\left(\frac{\dot{\varepsilon}}{\dot{\varepsilon_0}}\right)+1\right] \quad (2)$$

The values for σ_2 and τ_6 were then determined by the transformation:

$$\dot{\sigma_i} = \sigma_i f^y(\dot{\varepsilon})^{-1}$$

$$\sigma_i = \sigma_2, \tau_6$$

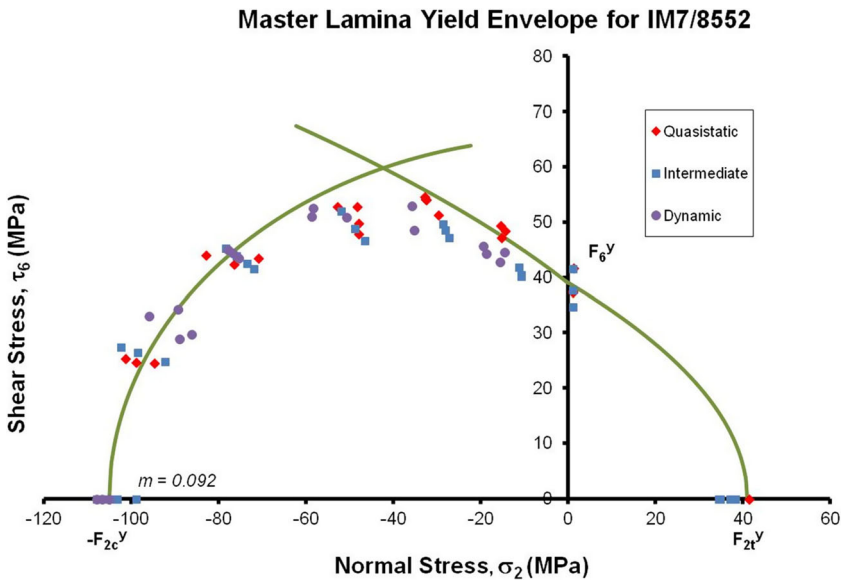

Fig. 6 Master lamina yield envelope

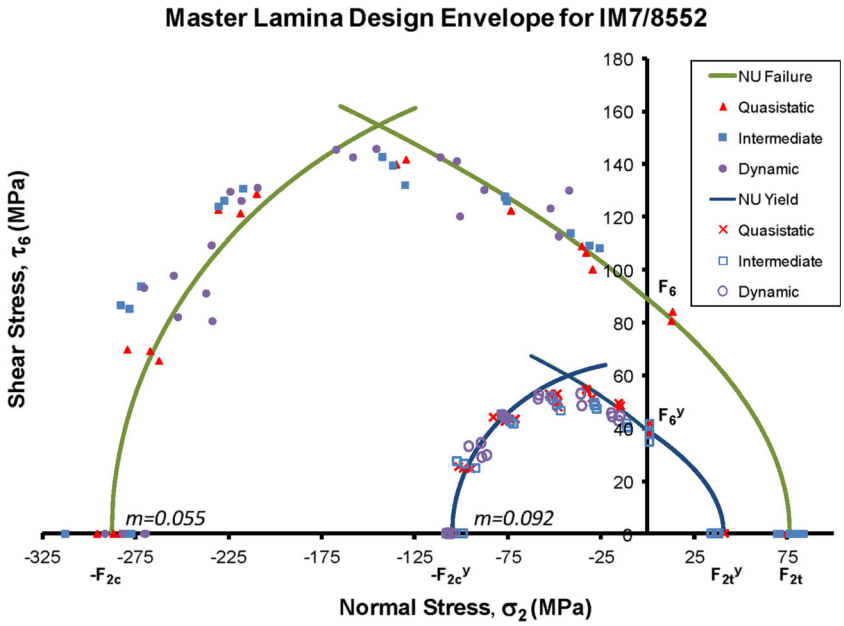

Fig. 7 Master NU lamina design envelopes

The off-axis uniaxial yield stresses were transformed using the standard transformation relations and plotted on the σ_2 - τ_6 plane (Fig. 4). The NU Yield Criteria and those obtained from classic failure theories are plotted for comparison.

The NU Yield Criteria are in superior agreement with the experimental data compared to classic theories (expressed in terms of yield criteria). The Sun theory provides a similarly good prediction for yielding; however, a fitting parameter independent of material properties is required to enhance the fit. The values for F_{2c}^{y}, F_{2t}^{y}, F_6^{y}, E_2, and G_{12} obtained from the intermediate and dynamic rate experiments were used for the corresponding yield envelopes. However, in the case of F_{2t}^{y} and F_6^{y} properties, the high rate values were obtained by extrapolation due to experimental limitations. The results are shown in Fig. 5**.** The intermediate and dynamic strain rate envelopes again are in good agreement with the experimental results in the σ_2 - τ_6 plane.

The strain rate dependence relation (1) was used with $m = 0.092$ to produce a master data set which was compared with the NU master yield envelope, as shown in Fig. 6.

The NU Yield Criteria fit the data for each of the tested strain rates (10^{-4}, 1, 10^3 s^{-1}) well, and provide an additionally useful tool for design. Considering that the same testing done to determine the strength values F_{2c}, F_{2t}, F_6 may be used to also obtain the yield stresses F_{2c}^{y}, F_{2t}^{y}, and F_6^{y}, this material knowledge comes at no additional experimental cost. The master normalized lamina ultimate failure data from [17] and the angle-ply yield data from the current investigation were integrated to create a master 'design envelope', shown in Fig. 7.

The combined master yield and ultimate lamina failure envelopes create a unique design plot. The plot provides a designer or structural analyst with ample flexibility for considering the strain rate effects on the failure as well as the yielding for a particular lamina orientation. Thus, the NU Failure Theory and the NU Yield Criteria may be simply used for determining these key material properties. Further details are provided in the work of Daniel et al. [24].

Table 3 Thermally induced residual stresses in ply of angle-ply laminate

[±θ]	σ_{1res} (MPa)	σ_{2res} (MPa)	τ_{6res} (MPa)
15	−7.2	7.2	−12.4
30	−25.9	25.9	−15
45	−38.6	38.6	0
60	−25.9	25.9	15
75	−7.2	7.2	12.4

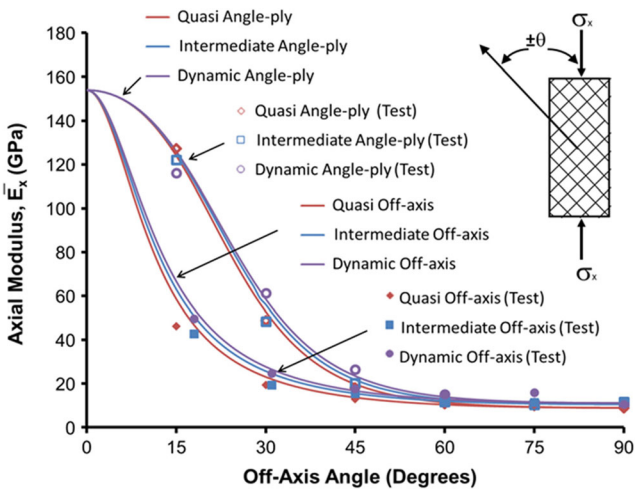

Fig. 8 Axial moduli for unidirectional lamina and angle-ply laminates

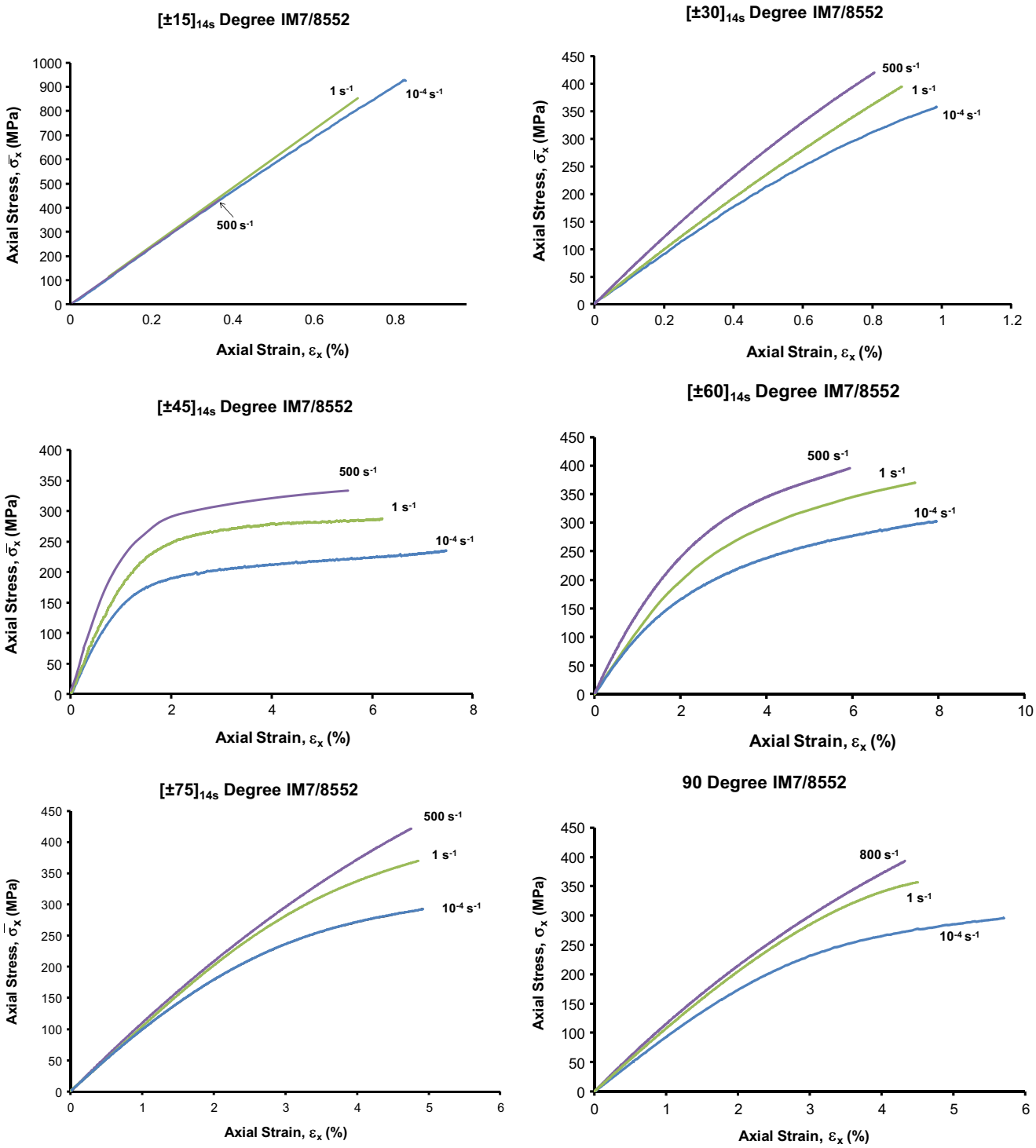

Fig. 9 Angle-ply axial stress behavior at quasi-static, intermediate, and dynamic strain rates

Angle-Ply Laminate Failure

To validate the NU Yield Criteria, it is required to isolate the underlying theoretical assumptions in more hierarchically complex scenarios for evaluation. In this light, new angle-ply laminates, $[\pm\theta]_{14s}$ (where $\pm\,\theta = 15°, 30°, 45°, 60°, 75°, 90°$), were manufactured from the same IM7/8552 tape system and tested under uniaxial compression to provide a comprehensive dataset to evaluate yield response. Laminate configuration was limited to a single ply for each orientation during layup (i.e.no ply grouping) to minimize the effect of edge interlaminar stresses [25]. The ±90° laminate is simply a unidirectional plate tested in the direction transverse to the fibers. Cuntze [26] relates that the matrix-dominated 'inter-

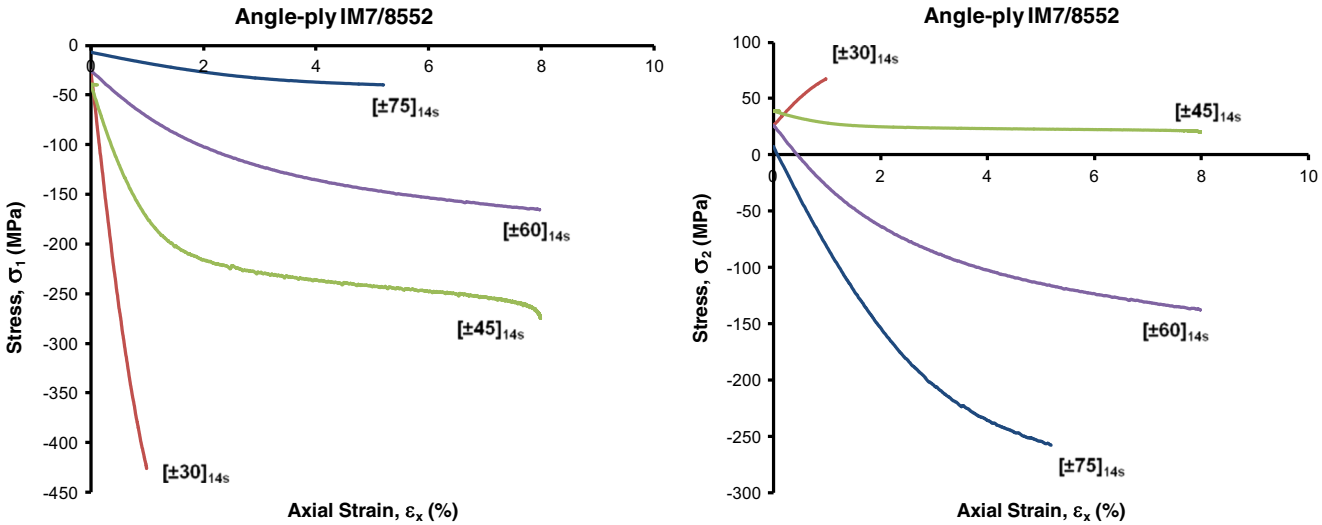

Fig. 10 Influence of thermally induced residual stresses in angle-ply laminates

fiber' failure modes present in such laminates are those least-well modeled by the leading theories in the recent worldwide failure exercises (WWFE), and Jadhav et al. [27] noted the potential for significant strain-rate-dependence for such modes in angle-ply laminates of a similar material system.

Angle-Ply Thermal Residual Stresses

To determine the thermally-induced residual cure stresses, the temperature difference (ΔT) between ambient temperature and the curing stress-free temperature was determined to be −150 K [28]. Additionally, the in-situ ply stress relations were derived to include the thermally-induced residual stresses (σ_{1res}, σ_{2res}, τ_{6res}):

$$\sigma_1 = \sigma_x\left[Q_{11}\left(\frac{m^2}{Q_{xx}-\frac{Q_{xy}^2}{Q_{yy}}}-\frac{n^2Q_{yx}}{Q_{yy}Q_{xx}-Q_{xy}^2}\right)+Q_{12}\left(\frac{n^2}{Q_{xx}-\frac{Q_{xy}^2}{Q_{yy}}}-\frac{m^2Q_{yx}}{Q_{yy}Q_{xx}-Q_{xy}^2}\right)\right]+\sigma_{1res} \tag{3}$$

Table 4 Yield stresses of angle-ply laminates under compression at quasi-static, intermediate, and dynamic strain rates

$[\pm\theta]_{14s}$	10^{-4} s^{-1} (MPa)	1 s^{-1} (MPa)	500 s^{-1} (MPa)
90	105	146 [3]	175 [2.4]
75	97 [1.8]	133 [7.5]	160 [6.4]
60	46 [2.8]	75 [5.8]	113 [10.9]
45	40	60	94 [6.8]
30	120 [4.8]	130 [2.4]	182 [11.4]
15	540 [9.8]	700	–

$$\sigma_2 = \sigma_x\left[Q_{21}\left(\frac{m^2}{Q_{xx}-\frac{Q_{xy}^2}{Q_{yy}}}-\frac{n^2Q_{yx}}{Q_{yy}Q_{xx}-Q_{xy}^2}\right)+Q_{22}\left(\frac{n^2}{Q_{xx}-\frac{Q_{xy}^2}{Q_{yy}}}-\frac{m^2Q_{yx}}{Q_{yy}Q_{xx}-Q_{xy}^2}\right)\right]+\sigma_{2res} \tag{4}$$

$$\tau_6 = -2mnQ_{66}\sigma_x\left[\frac{1}{Q_{xx}-\frac{Q_{xy}^2}{Q_{yy}}}+\frac{Q_{yx}}{Q_{yy}Q_{xx}-Q_{xy}^2}\right]+\tau_{6res} \tag{5}$$

where $m = cos\theta$, $n = sin\theta$, and σ_x is the axial stress.

The in-situ ply thermal residual stresses are provided in Table 3.

The axial angle-ply laminate moduli were determined using lamination mechanics for symmetric balanced laminates [28]. The axial Young's modulus is related to the in-plane laminate stiffness, [A], and thickness, h, as follows:

$$\overline{E_x} = \frac{1}{h}\left[A_{xx}-\frac{A_{xy}^2}{A_{yy}}\right] \tag{6}$$

which reduces to a relation in terms of the reduced lamina stiffnesses, [Q]:

$$\overline{E_x} = \left[Q_{xx}-\frac{Q_{xy}^2}{Q_{yy}}\right] \tag{7}$$

The axial moduli of the angle-ply laminate were plotted against axial strain; the average off-axis lamina axial moduli are included for comparison in Fig. 8.

The predicted values were in good agreement with the experimentally obtained data. In the figure, a clear correlation exists between the fiber orientation and composite moduli, as the fibers more effectively carry the load when they are closely

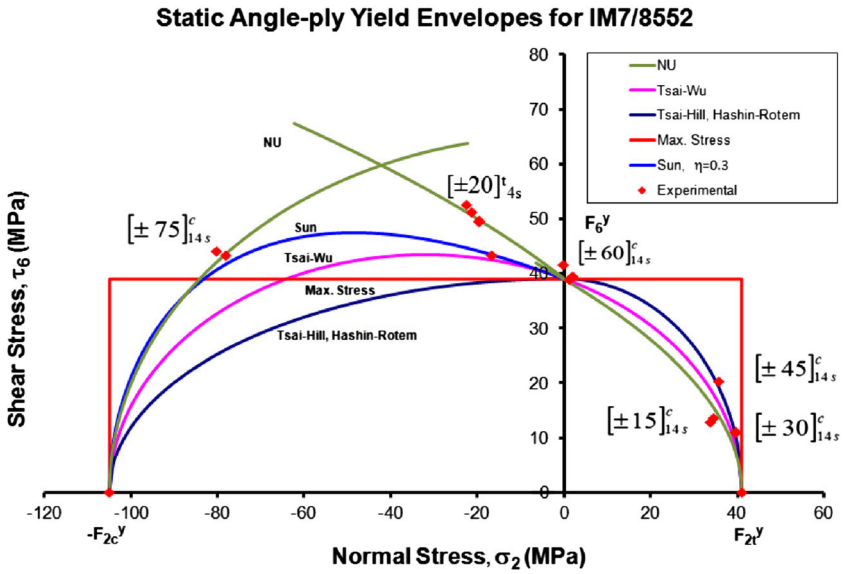

Fig. 11 Comparison of static angle-ply yield envelopes for IM7/8552; compression (c) and tension (t) noted with $[\pm 20]^{t}_{4s}$ data [25]

aligned with the loading axis. A transition from the 'fiber-dominated' to the 'matrix-dominated' moduli is seen to occur between 45° and 50°. Angle-ply stress-strain behavior was recorded using the same approach as that for the lamina at three strain rates [17], and the bar-calculated and measured strain gage strain-time history for a ± 45° specimen is shown in Fig. 2. The results are shown in Fig. 9.

The angle-ply maximum stress increases with increasing strain rate while the maximum strain decreases; this is considered a 'stiffening' and 'strengthening' effect. The σ_1 and σ_2 stress-strain behavior for the $[\pm 30]_{14s}$, $[\pm 45]_{14s}$, $[\pm 60]_{14s}$, and $[\pm 75]_{14s}$ laminates is shown in Fig. 10.

The transverse stress provides an interesting perspective on the transition from tensile to compressive loading experienced by the laminate as the orientation changes from ±30° to ±45°. The results in Fig. 9 indicated a significant contrast in strain to failure between these two orientations and insight into why this occurs is shown in Fig. 10. The ±30° laminate experiences tensile stress in the transverse direction for the axial compressive loading condition; the ultimate failure stress and strain correspond closely to the thresholds set by F_{2t} and ε_{2t}. A key observation is that the residual stress for this laminate is quite large (~26 MPa) compared to F_{2t} (76.4 MPa).

Strain-Rate-Dependence of Angle-Ply Laminate Yielding

The yield points were obtained from the angle-ply laminate stress-strain curves (Fig. 10) and are provided in Table 4.

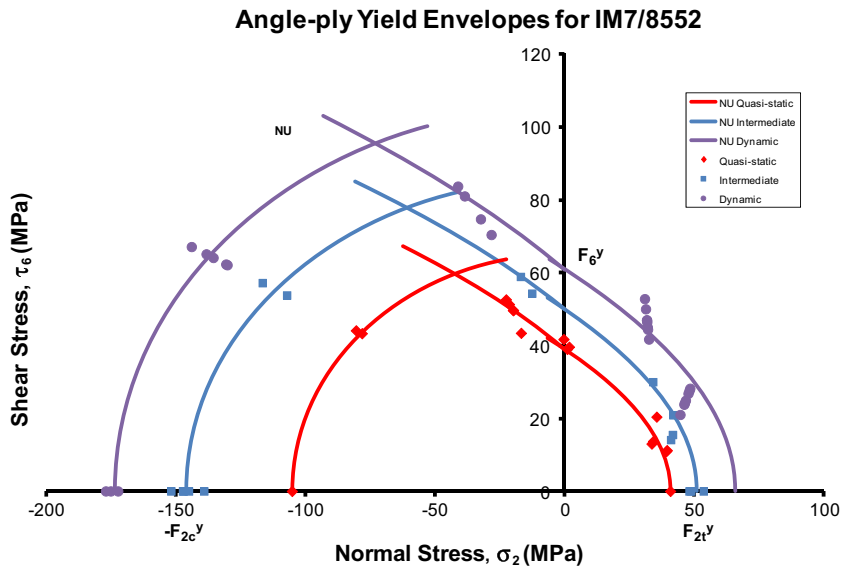

Fig. 12 Yield envelopes for IM7/8552 angle-ply laminates for quasi-static, intermediate and dynamic strain rates

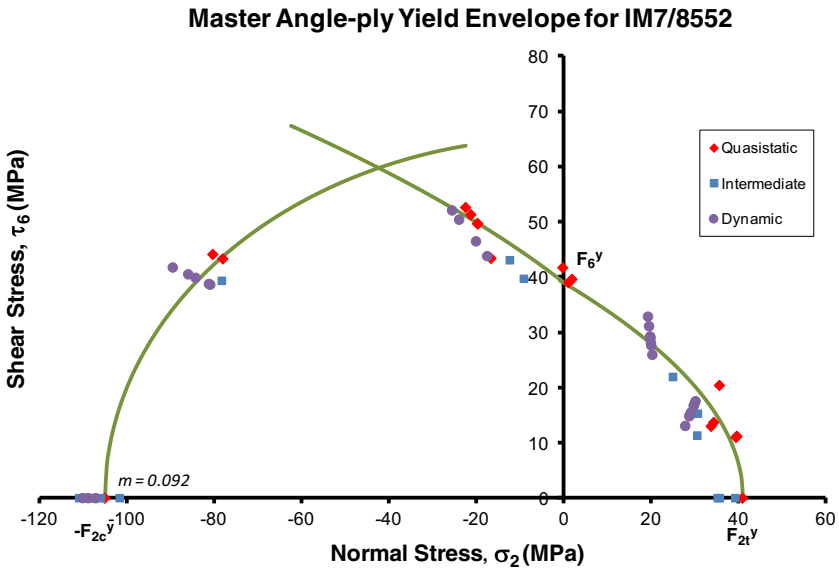

Fig. 13 Master angle-ply laminate yield envelope

Due to premature failure, the yield stress for the $[\pm 15]_{14s}$ laminate was not obtained at the high strain rate. In the other cases, the yield stress was seen to increase with increasing strain rate. Compared to the unidirectional lamina, the corresponding angle-ply laminates are shown to yield at a lower applied axial stress. This behavior is due to the biaxial state of stress as well as the 'locked-in' residual stresses from curing. The axial stress at yielding was used to determine the corresponding lamina stresses using lamination theory and the residual stresses for $\Delta T = -150\ K$. Testing of angle-ply laminates ranged from $[90]_{54}$ (lamina) in compression, through $[\pm\theta]_{14s}$, to $[90]_{16}$ in tension. The Northwestern lamina Yield Criteria presented previously were applied and the yield data were plotted and compared with those of the classical failure theories. The static angle-ply yield envelope is depicted in Fig. 11, which includes $[\pm 20]^t_{4s}$ (tension) data from Werner et al. [25], and all three yield envelopes are shown in Fig. 12.

Importantly, the strain rate dependence of the angle-ply laminates is the same as that of the lamina according to relation (1) with $m = 0.092$. The data was normalized in terms of the static reference strain rate and plotted in Fig. 13 with the master NU Yield envelope.

The master NU Yield envelope fits the experimental data quite well. Importantly, the lamina and angle-ply data may be combined into a single yield envelope as shown in Fig. 14.

Thus, from a single set of lamina tests the strain-rate-dependent yield behavior of angle-ply laminates may be predicted with enhanced accuracy using a limited and efficient testing framework. With the present NU Criteria and framework, it is proposed that a limited set of tests may be

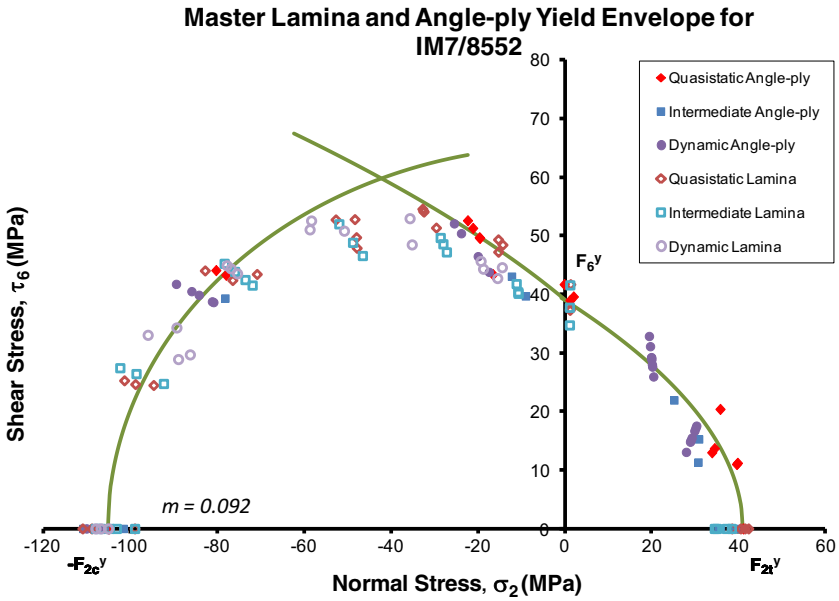

Fig. 14 Master NU lamina and angle-ply laminate yield envelopes for IM7/8552

performed to provide the required data for computational model validation. This is especially critical in the consideration of multi-scale analysis approaches wherein element formulations must be validated based on piecewise capability [3].

Conclusion

This investigation provides a direct benchmark by which to evaluate the Northwestern Yield Criteria for a lamina and the validity of their application to composite laminates. The results indicate that the failure-mode-based Northwestern Failure Theory may be recast as a set of yield criteria to effectively predict the yielding of both lamina and angle-ply laminates. The presented approach reduces the number of required characterization tests by an order of magnitude; furthermore, it provides both the design engineer and structural analyst key insight into composite laminate behavior. Utilizing the NU Yield Criteria and NU Failure Theory, it has been shown that an analyst may efficiently and effectively validate underlying modeling assumptions for matrix damage initiation and propagation within a lamina and laminate. Investigation of neat matrix strain-rate-dependence in light of the NU Yield Criteria is currently in progress.

Acknowledgements The work described in this paper was sponsored by the Office of Naval Research (ONR). The authors are grateful to Dr. Y.D.S. Rajapakse of ONR for his encouragement and cooperation.

References

1. ASME. Guide for Verification and Validation in Computational Solid Mechanics. ASME V&V 10. 2006:1–36
2. Hart-Smith LJ (1993) The role of biaxial stresses in discriminating between meaningful and illusory composite failure theories. Compos Struct 25:3–20
3. Razi H, Schaefer JD, Wanthal S (2016) Rapid Integration of New Analysis Methods in Production, 31st ASC Technical Conference and ASTM D30 Meeting
4. Arguelles A, Vina J, Canteli AF (2011) Influence of the matrix type on the mode I fracture of carbon-epoxy composites under dynamic delamination. Exp Mech 51(3):293–301
5. Costa ML, Botelho EC (2005) Paiva JMFd, Rezende MC. Characterization of cure of carbon/epoxy Prepreg used in aerospace field. Mater Res 8(3):317–322
6. Eibl S (2008) Observing Inhomogeneity of Plastic Components in Carbon Fiber Reinforced Polymer Materials by ATR-FTIR Spectroscopy in the Micrometer Scale. J Compos Mater 42(12): 1231–1246
7. Lee J, Soutis C (2007) A study on the compressive strength of thick carbon fibre–epoxy laminates. Compos Sci Technol 67(10):2015–2026
8. Marasco AI, Cartié DDR, Partridge IK, Rezai A (2006) Mechanical properties balance in novel Z-pinned sandwich panels: out-of-plane properties. Compos A: Appl Sci Manuf 37(2):295–302
9. Murri GB (2013) Evaluation of delamination onset and growth characterization methods under mode I fatigue loading. NASA/TM-2013-217966
10. Tsotsis TK, Keller S, Lee K, Bardis J, Bish J (2001) Aging of polymeric composite specimens for 5000 hours at elevated pressure and temperature. Compos Sci Technol 61(1):75–86
11. Wolfrum J, Eibl S, Lietch L (2009) Rapid evaluation of long-term thermal degradation of carbon fibre epoxy composites. Compos Sci Technol 69(3–4):523–530
12. NIAR, NCAMP. Hexcel 8552 IM7 Unidirectional Prepreg 190 gsm & 35% RC Qualification Material Property Data Report. 2011 April 22, 2011;CAM-RP-2009-015(Rev A)
13. Daniel IM, Luo J-J, Schubel PM, Werner BT (2009) Interfiber/interlaminar failure of composites under multi-axial states of stress. Compos Sci Technol 69(6):764–771
14. Daniel IM, Cho J-M, Werner BT, Fenner JS (2011) Characterization and Constitutive Modeling of Composite Materials Under Static and Dynamic Loading. AIAA J 49(8):1658–1664
15. Daniel IM, Werner BT, Fenner JS (2011) Strain-rate-dependent failure criteria for composites. Compos Sci Technol 71(3):357–364
16. Werner BT, Daniel IM (2012) Characterization and modeling of polymeric matrix under static and dynamic loading. SEM XII International Congress & Exposition on Experimental & Applied Mechanics 2012. Costa Mesa, CA
17. Schaefer JD, Werner BT, Daniel IM (2014) Strain-Rate-Dependent Failure of a Toughened Matrix Composite. Exp Mech 54(6):11–20
18. Karim MR, Fatt MSH (2006) Rate-dependent constitutive equations for carbon fiber-reinforced epoxy. Polym Compos 27(5): 513–528
19. Koerber H, Camanho PP (2011) High strain rate characterisation of unidirectional carbon–epoxy IM7-8552 in longitudinal compression. Compos A: Appl Sci Manuf 42(5):462–470
20. Thiruppukuzhi SV, Sun CT (2001) Models for the strain-rate-dependent behavior of polymer composites. Compos Sci Technol 61(1):1–12
21. Catalanotti G, Camanho PP, Marques AT (2013) Three-dimensional failure criteria for fiber-reinforced laminates. Compos Struct 95(0): 63–79
22. Werner BT, Daniel IM (2014) Characterization and modeling of polymeric matrix under multi-axial static and dynamic loading. Compos Sci Technol 102:113–119
23. Schaefer JD (2014) Matrix dominated failure of fiber-reinforced composite laminates under static and dynamic loading. Northwestern University, Dissertation
24. Daniel IM, Schaefer JD, Werner B (2015) Yield criteria for matrix and composite materials under static and dynamic loading, 20th international conference on composite materials, July 19-24
25. Werner BT, Schaefer JD, Daniel IM (2013) Effect of Ply Dispersion on Failure Characteristics of Multidirectional Laminates. SEM 2013 Annual Conference & Exposition on Experimental and Applied Mechanics; June 3–5; Lombard, IL2013
26. Cuntze RG (2004) The predictive capability of failure mode concept-based strength criteria for multi-directional laminates—part B. Compos Sci Technol 64(3–4):487–516
27. Jadhav A, Woldesenbet E, Pang S-S (2003) High strain rate properties of balanced angle-ply graphite/epoxy composites. Compos Part B 34(4):339–346
28. Daniel IM, Ishai O (2006) Engineering mechanics of composite materials. Oxford University Press, Oxford, New York